Algorithm for computing holographic optical tweezers at video rates

Mario Montes-Usategui*, Encarnación Pleguezuelos, Jordi Andilla, Estela Martín-Badosa, and Ignasi Juvells
Grup de Recerca en Òptica Física, Departament de Física Aplicada i Òptica, Universitat de Barcelona, Martí i Franquès 1, Barcelona 08028, Spain

ABSTRACT

Digital holography enables the creation of multiple optical traps at arbitrary three-dimensional locations and spatial light modulators permit updating those holograms at video rates. However, the time required for computing the holograms makes interactive optical manipulation of several samples difficult to achieve. We introduce an algorithm for computing holographic optical tweezers that is both easy to implement and capable of speeds in excess of 10 Hz when running on a Pentium IV computer. A discussion of the pros and cons of the algorithm, a mathematical analysis of the efficiency of the resulting traps, as well as results of the three-dimensional manipulation of polystyrene micro spheres are included.

Keywords: Digital holography, phase-only filters and kinoforms, spatial light modulators, optical tweezers.

1. INTRODUCTION

Fast computation of holograms is a prerequisite for building interactive holographic optical manipulation systems. Unfortunately, the nonlinear and usually non-analytic relations between a hologram displayed onto a spatial light modulator and its corresponding reconstruction at the sample plane make the use of iterative, computational intensive algorithms often necessary [1-3]. Although fast manipulation is still feasible by computing the holograms off-line and then displaying them at video rates, only movements with pre-defined trajectories are then possible. Thus, interaction with a potential human operator needs real-time generation of holograms through faster algorithms [4-8] or by means of more powerful computing platforms, such as the graphic processing units of modern graphics boards [9,10].

As a matter of fact, rapid generation of optical traps can be achieved by alternate methods, which require no computation. For example, time-sharing the laser between traps [11] is a powerful, flexible and inexpensive possibility. However, in high-precision applications, the number of trapping sites needs to be small (4-6) [12] since the laser shifts prevent accurate measurements of applied force. Also, positioning and movement is limited only to two dimensions. The generalized phase contrast method [13] provides an instant conversion between phase and intensity and is therefore well suited to quickly generate optical traps with spatial light modulators (SLMs), through a frequency-filtering, all-optical, non-holographic approach. Nevertheless, the imaging nature of the setup makes it difficult to control the samples in three-dimensions [14].

Fresnel diffraction can be used to advantage [15] in real-time steering of optical tweezers since movement of the hologram on the computer screen translates into a similar movement of the corresponding trap. On the negative side, there seems to be a trade-off among trap efficiency, range of allowed movements and number of simultaneous traps because of the limited real state available on the SLM to display the holograms. In our opinion, all these methods lack the simplicity and universality of the traditional holographic approach.

This communication addresses the problem of the high computational load of most existing algorithms and presents a low-cost solution based on the random mask encoding technique of multiplexing phase-only filters [16]. The result is a direct, non-iterative and extremely fast algorithm that can be used for computing arbitrary arrays of optical traps. Additional benefits include the possibility of modifying any existing hologram to quickly add more trapping sites and the inexistence of ghost traps or replicas. The main drawback of the method is a reduced efficiency, being more suitable to generate a small number of optical traps. We have implemented the procedure on a Pentium IV personal computer and achieved frame rates in excess of 10 Hz with little code optimization. A Java front end allows the user to interactively manipulate microscopic samples just by clicking and dragging on a computer screen.

*mario_montes@ub.edu; www.ub.edu/optics

2. EXPERIMENTAL SETUP

Our experimental setup is shown in Fig. 1. It is very similar to that discussed in detail in Ref. 17 except for the microscope, which has been upgraded to a higher quality instrument.

A continuous-wave, frequency-doubled Nd:YVO_4 laser beam (Viasho Technology, λ=532 nm, 120 mW) is expanded by a spatial filter, collimated by lens L1 and linearly polarized by a high quality polarizer. It illuminates a twisted-nematic liquid-crystal spatial light modulator (Holoeye Photonics, LC-R 2500) sandwiched between a half-wave plate and an analyzer with the proper orientations to achieve phase-only modulation [17]. Interestingly, the Holoeye SLM is a reflective device and we place it tilted 45º with respect to the incident beam (see Figure 2). The usual configuration for a reflective modulator is to place it perpendicular to the optical axis and then redirect the beam out with a beam-splitter. However, the control of the input and output polarization is a much convenient feature of the setup as it allows free access to the different operating modes of the device (such as the phase-only modulation operating curve). Both constraints, polarization control and on-axis operation, can be met by the use of a non-polarizing beam-splitter but the round trip path through that element would result in a loss of 75% of the incident light. This is unacceptable considering the large power required for trapping even a small number of samples, so we discarded that possibility in favor of that shown in Figure 2. It is also very convenient from the point of view of arranging the whole optical setup and we have found that, although not lying on a plane perpendicular to the axis, the SLM is capable of producing fairly good traps.

Light finally enters an inverted microscope (Nikon Eclipse TE-2000E) through the fluorescence port and is reflected upwards by a dichroic mirror (Chroma Technology) to an oil-immersion, high numerical aperture, objective (Nikon Plan Fluor 100x, 1.30 NA). Lenses L2 and L3 (which is inside the microscope, attached to the fluorescence cube that contains the dichroic), image the SLM onto the exit pupil of the microscope objective to prevent vignetting of high frequency Fourier components [2,3]. They are arranged to form a telescope so as to still provide parallel illumination to the infinity-corrected objective. Finally, a CCD camera (Qimaging QICAM 1394) allows observation and recording of the experiments.

Since the spatial light modulator is illuminated by collimated light and the diffracted beams are observed at the focal plane of the objective lens (focal length, *f'*), the relation between the complex reflectance, *R(u,v)*, of the modulator and the electric field at the observation plane, *E(x,y)*, is, except for irrelevant phase terms [18], that of a Fourier transform:

$$E(x,y) = \iint R(u,v) e^{-i\frac{2\pi}{\lambda f'}(ux+vy)} du dv \,. \tag{1}$$

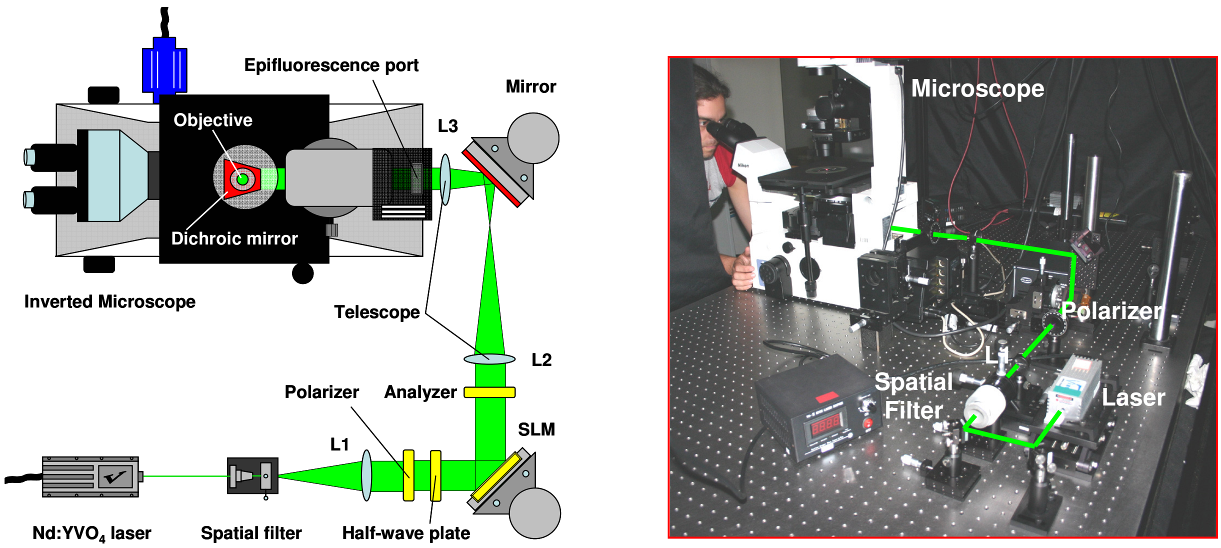

Fig. 1. Optical setup for generating holographic optical tweezers

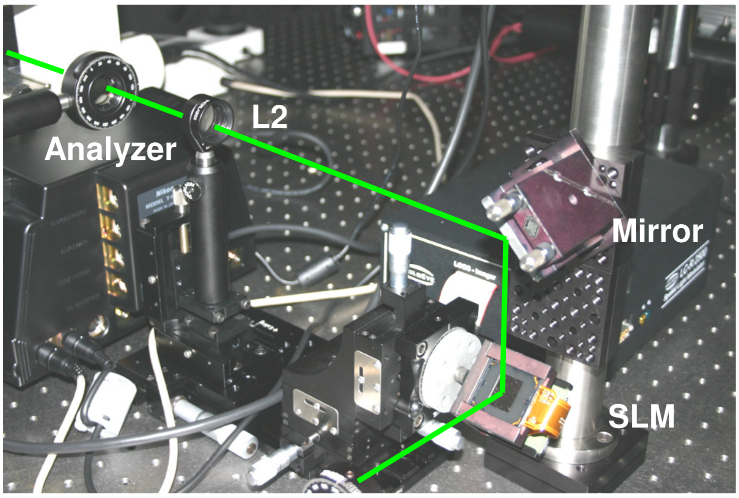

Fig. 2. Holoeye reflective spatial light modulator tilted 45º with respect to the optical axis

3. ALGORITHM

Given Eq. (1) above, when the spatial light modulator displays the hologram:

$$R(u,v)=\sum_{k=1}^{N} e^{i\frac{2\pi}{\lambda f'}(x_k u+y_k v)} , \tag{2}$$

a set of N off-axis traps will appear at positions (x_k, y_k) on the sample plane, according to:

$$E(x,y)=\sum_{k=1}^{N}\iint e^{-i\frac{2\pi}{\lambda f'}[(x-x_k)u+(y-y_k)v]}dudv=\sum_{k=1}^{N}\delta(x-x_k, y-y_k). \tag{3}$$

Hologram $R(u,v)$ is the superposition of N linear phase functions with slopes (x_k, y_k). Unfortunately, $R(u,v)$ is not a pure phase function and cannot be directly displayed on a modulator working in a phase-only configuration. Therefore, this problem needs to be solved if optical tweezers arrays by means of holographic optical elements on spatial light modulators are to be generated. The algorithms [1-6] try to find a hologram that, being a phase function, does not deviate significantly from the expected goal, that of producing the desired trap array. Such algorithms are usually iterative and computationally expensive.

Our solution is non-iterative. It is an adaptation of the random-mask encoding technique [7, 16] to this particular problem and consists of the multiplication of the linear phase functions in Eq. (2) by spatially disjoint binary masks, i.e.:

$$R(u,v)=\sum_{k=1}^{N} h_k(u,v) e^{i\frac{2\pi}{\lambda f'}(x_k u+y_k v)} , \tag{4}$$

where

$$h_k(u,v)=\begin{cases}1 & iff\ (u,v)\in I_k \\ 0 & otherwise\end{cases} , \tag{5}$$

with

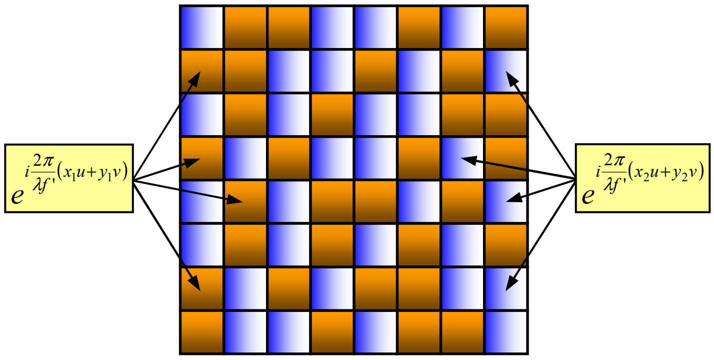

Fig. 3. Encoding two linear phases by complementary random binary masks.

$$I_l \cap I_m = \varnothing \quad \forall\, l,m \,\middle|\, l \neq m \quad and \quad \bigcup_{k=1}^{N} I_k = \Re^2 \,. \tag{6}$$

That is, the method involves dividing the spatial light modulator into as many subdomains, I_k, as traps are required so that these subdomains do not overlap and jointly cover the whole modulator area. Then, each linear phase function is displayed only on the pixels of a given I_k. (see Fig. 3).

With this arrangement, $R(u,v)$ is trivially a pure phase function with no further modification. Applying the convolution theorem [18] and Eq. (3), the field at the sample plane is:

$$E(x,y) = \sum_{k=1}^{N} H_k\left(x - x_k, y - y_k\right), \tag{7}$$

where $H_k(x,y)$ is the Fourier Transform of $h_k(u,v)$. Thus, function $H_k(x,y)$ appears centered at position (x_k,y_k). If the binary masks are selected such that their Fourier transforms $H_k(x,y)$ consist of a single peak with flat sidelobes, then E(x,y) will be a good approximation to the desired array of optical traps. Random masks, as proposed in Ref. 16, give good results in this respect. For example, Fig. 4(a) shows a random binary mask with 50% of its pixels set to one and the remaining 50% to zero. Fig. 4(b) shows the magnitude squared of its Fourier transform, a sharp peak on a small random background. The scale on the Z axis is logarithmic so as better to show small intensity features, since the background is five orders of magnitude lower than the central peak.

Fig. 5 shows a comparison between the experimental results of this algorithm and those obtained by the "gratings and lenses" algorithm [6,8]. Notice the absence of ghost traps in Fig. 5(a) since off-trap energy tends to scatter over the whole sample plane, instead of concentrating at specific locations (giving undesired trapping sites, such as those in Fig. 5(b)).

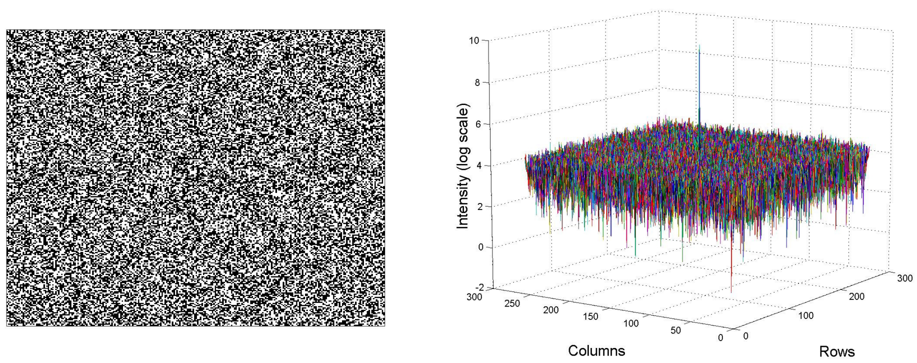

a) b)

Fig. 4. a) Binary mask, 256x256 pixels. b) Magnitude squared of its Fourier transform (log scale).

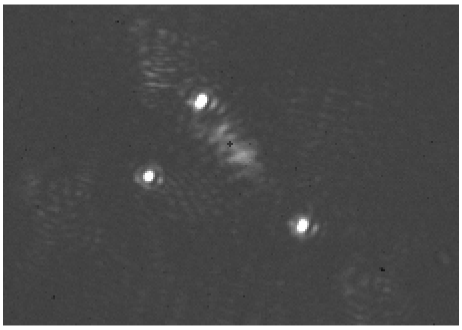

a)

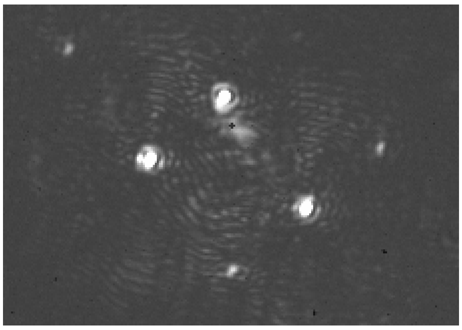

b)

Fig. 5. Three traps produced by the "random mask" (a) and the "gratings and lenses" (b) algorithms, respectively.

Also, Figure 5 shows the main drawback of our algorithm, a lower efficiency. The three traps in Fig. 5(a) are substantially less energetic than those in Fig. 5(b). In fact, the random mask encoding technique lends itself easily to analysis in this regard:

Let us consider a hologram, *R(j,k)*, of *NxN* pixels designed to create *P* traps and let us assume, with no loss of generality, that is illuminated by a plane wave of unit amplitude, A=exp(iφ). The energy at a plane immediately after the hologram is:

$$E_{TOT} = \sum_{j=1}^{N}\sum_{k=1}^{N}\left(R(j,k)A\right)^{*} R(j,k)A = \sum_{j=1}^{N}\sum_{k=1}^{N}\left|R(j,k)\right|^{2} \ , \tag{8}$$

whence, since the hologram is a pure phase function, we have:

$$E_{TOT} = NxN = N^{2} \ , \tag{9}$$

which, by virtue of Parseval's theorem, is also the total energy at the reconstruction plane.

On the other hand, the field amplitude at the *m*th trap position, (r_m,s_m), can be written, in discrete notation, as:

$$\begin{aligned} C(r_m,s_m) &= \frac{1}{N}\sum_{j=1}^{N}\sum_{k=1}^{N} R(j,k)\exp\left[-i\frac{2\pi}{N}(r_m j + s_m k)\right] = \\ &= \frac{1}{N}\sum_{j=1}^{N}\sum_{k=1}^{N}\sum_{l=1}^{P} h_l(j,k)\exp\left\{-i\frac{2\pi}{N}\left[(r_m - r_l)j + (s_m - s_l)k\right]\right\} \approx \frac{1}{N}\sum_{j=1}^{N}\sum_{k=1}^{N} h_m(j,k) = \frac{1}{N}\frac{N^2}{P} = \frac{N}{P} \ . \end{aligned} \tag{10}$$

where *R(j,k)* represents the hologram and $h_l(j,k)$ the *l*th random binary mask.

Therefore, the total energy reaching the *P* traps is:

$$E_{TRAPS} \approx Px\left(\frac{N}{P}\right)^{2} = \frac{N^{2}}{P} \ , \tag{11}$$

whence, the efficiency of the hologram finally takes the form:

$$Efficiency = \frac{E_{TRAPS}}{E_{TOT}} \approx \left(\frac{N^{2}/P}{N^{2}}\right) = \frac{1}{P} \ . \tag{12}$$

4. ADDITIONAL USEFUL PROPERTIES

This procedure shows some useful features that we comment on below.

a) Intensity control

The intensity of optical traps generated by the algorithm shows a remarkable uniformity for a small number of traps. For example, in our experiments we have found maximum variations in intensity of less than 4% for arrays of 2x2 optical traps (512x512 pixel holograms). However, for larger arrays (6x6) the intensity variations may increase up to 25%. When this is a problem or if the optical traps have to be of different intensity, a slightly more elaborate algorithm needs to be used [16]. Masks corresponding to traps that are required to be brighter are selected with a somewhat larger pixel count at the expense of other masks (those corresponding to traps need to be weaker).

b) Incremental updating and hologram multiplexing

Contrary to other algorithms, all information is very well localized within the binary masks so addition of new trapping sites can be done without recomputing the whole hologram. Specifically, for a hologram of N pixels that encode m traps, $N/[m(m+1)]$ pixels from each binary mask are randomly discarded. Then, the resulting $N/(m+1)$ pixels are used to codify the new linear phase. Only these latter pixels need to be updated.

Interestingly, this can be done over a hologram computed with any other algorithm, in which the information is distributed: discard a number of pixels and use them to produce a new trapping site with the random mask encoding technique. None of the existing traps is more affected than the others, the net effect is a lower-energy set of existing traps and a new trapping site at the desired location. This may be used to temporarily add a new trap to a pre-existing, higher-quality hologram, for example, for loading an array of optical traps with microscopic samples. Finally, the loading trap can be removed by restoring the original pixels.

Fig. 6 shows the result of adding a new trapping site to a hologram computed by the Gerchberg-Saxton algorithm [3,4,6] to produce an array of 2x2 optical traps. One fifth of its pixels were used to encode the new linear phase function. Again, the figure shows that the new trap is significantly less energetic than equivalent traps computed by the other algorithm. We are studying a possible solution to this low efficiency based on reducing the randomness of the binary masks (Fig. 7, simulated results).

Finally, two or more holograms can be multiplexed by multiplication of binary disjoint random masks to merge their individual properties into a single hologram.

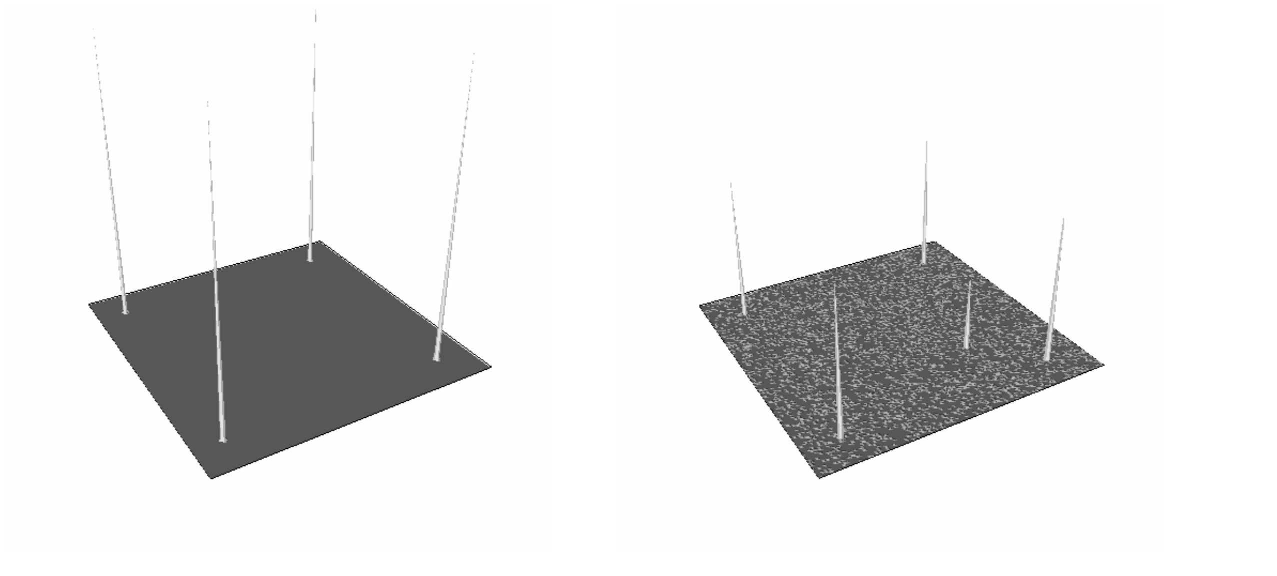

Fig. 6. Addition of a new trap to an already existing hologram.

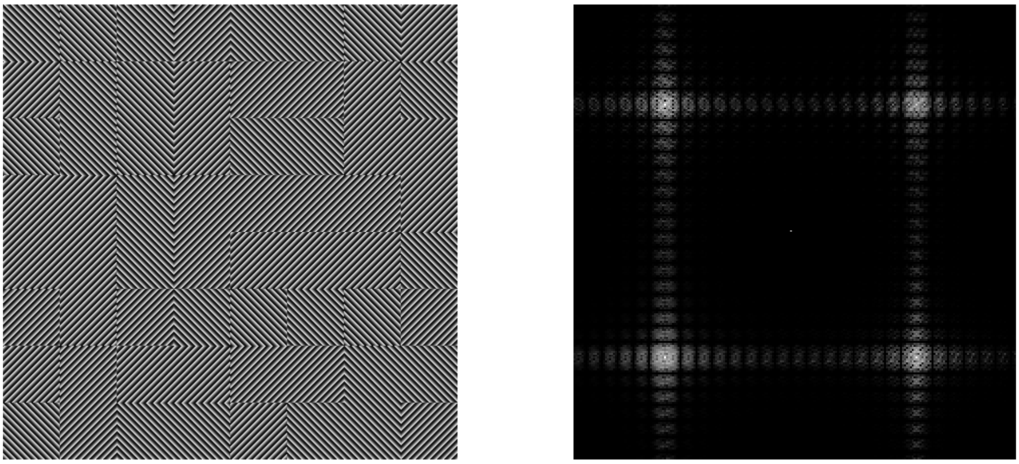

a) b)

Fig. 7. Modified hologram based on less random binary masks (a) and generated traps (b).

c) Speed

Once the random masks are selected, the hologram can be directly written onto the spatial light modulator with little extra computation. Thus, the procedure is very fast and can be easily carried out at near video-rates, therefore enabling real-time interaction with the user. We have developed an interactive holographic optical manipulation system based on this algorithm, as shown in the following image sequences (Figs. 8 and 9). The control software is implemented in Java and is capable of displaying holograms (512x512 pixels) at an average rate of 10-12 Hz (including aberration correction of the Holoeye SLM and compensation of the operating curve nonlinearities), using a Pentium IV HT, 3.2 Ghz, computer.

5. CONCLUSIONS

We propose a new procedure for the generation of holographic optical tweezers based on the random mask encoding technique. The result is a direct, non-iterative algorithm that has a number of positive features. Specifically, the algorithm is very fast and video-rate generation is easy to achieve. Moreover, the algorithm does not produce ghost traps and can be used to add further trapping sites to existing holograms, even those generated by other algorithms, without the need to re-compute them. Finally, the main limitation of this procedure seems to be hologram efficiency. We have shown that the efficiency, defined as the ratio between the energy of the traps to the total energy at the sample plane, decreases monotonically with increasing number of traps. Thus the algorithm seems suitable only to generate a small number of optical tweezers.

ACKNOWLEDGEMENTS

This work has been funded by the Spanish Ministry of Education and Science, under grants FIS2004-03450 and NAN2004-09348-C04-03.

REFERENCES

1. M. Reicherter, T. Haist, E. Wagemann, and H. Tiziani, "Optical particle trapping with computer-generated holograms written on a liquid-crystal display," Opt. Lett. **24**, 608-610 (1999).
2. D. G. Grier, "A revolution in optical manipulation," Nature **424**, 810-816 (2003).

3. J. E. Curtis, B. A. Koss, and D. G. Grier, “Dynamic holographic optical tweezers,” Opt. Commun. **207**, 169–175 (2002).
4. G. Sinclair, J. Leach, P. Jordan, G. Gibson, E. Yao, Z. J. Laczik, M. J. Padgett, and J. Courtial, "Interactive application in holographic optical tweezers of a multi-plane Gerchberg-Saxton algorithm for three-dimensional light shaping," Opt. Express **12,** 1665-1670 (2004).
5. M. Polin, K. Ladavac, S. Lee, Y. Roichman, and D. G. Grier, "Optimized holographic optical traps," Opt. Express **13,** 5831-5845 (2005).
6. J. Curtis, C. Schmitz, and J. Spatz, "Symmetry dependence of holograms for optical trapping," Opt. Lett. **30**, 2086-2088 (2005).
7. M. Montes-Usategui, E. Pleguezuelos, J. Andilla, and E. Martín-Badosa, "Fast generation of holographic optical tweezers by random mask encoding of Fourier components," Opt. Express **14**, 2101-2107 (2006).
8. J. Leach, K. Wulff, G. Sinclair, P. Jordan, J. Courtial, L. Thomson, G. Gibson, K. Karunwi, J. Cooper, Z. J. Laczik, and M. Padgett, "Interactive approach to optical tweezers control," Appl. Opt. **45**, 897-903 (2006).
9. N. Masuda, T. Ito, T. Tanaka, A. Shiraki, and T. Sugie, "Computer generated holography using a graphics processing unit," Opt. Express **14**, 603-608 (2006)
10. M. Reicherter, S. Zwick, T. Haist, C. Kohler, H. Tiziani, and W. Osten, "Fast digital hologram generation and adaptive force measurement in liquid-crystal-display-based holographic tweezers," Appl. Opt. **45**, 888-896 (2006)
11. K. Visscher, S. P. Gross, and S. M. Block “Construction of multiple-beam optical traps with nanometer-resolution position sensing,” IEEE J. Sel. Top. Quantum Electron. **2**, 1066-1076 (1996).
12. Guilford, W.H., J.A. Tournas, D. Dascalu, and D.S. Watson, “Creating multiple, time-shared laser traps with simultaneous displacement detection using digital signal processing hardware.” Anal. Biochem. **326**, 153-166 (2004).
13. R. Eriksen, P. Mogensen, and J. Glückstad, "Multiple-beam optical tweezers generated by the generalized phase-contrast method," Opt. Lett. **27**, 267-269 (2002).
14. P. J. Rodrigo, V. R. Daria, and J. Glückstad, “Four-dimensional optical manipulation of colloidal particles,” Appl. Phys. Lett. **86**, 074103 (2005).
15. A. Jesacher, S. Fürhapter, S. Bernet, and M. Ritsch-Marte, "Diffractive optical tweezers in the Fresnel regime," Opt. Express **12**, 2243-2250 (2004)
16. J. Davis and D. Cottrell, "Random mask encoding of multiplexed phase-only and binary phase-only filters," Opt. Lett. **19**, 496-498 (1994).
17. E. Pleguezuelos, J. Andilla, A. Carnicer, E. Martín-Badosa, S. Vallmitjana, and M. Montes-Usategui, “Design of a low-cost, interactive, holographic optical tweezers system,” Proc of SPIE, this same volume.
18. J. W. Goodman, *Introduction to Fourier Optics* (McGraw-Hill, 1996).

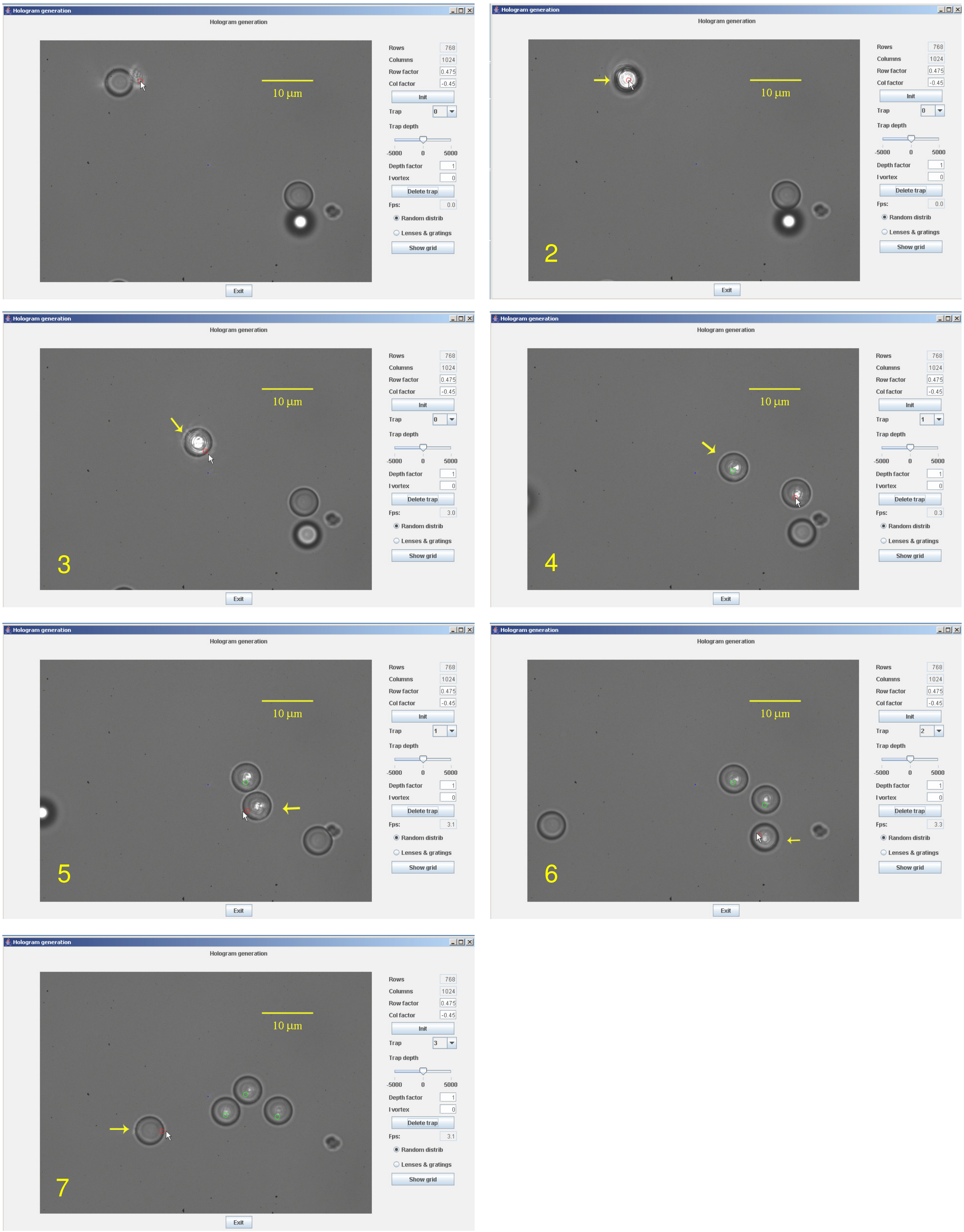

Fig. 8. Sequence of images showing the trapping and manipulation of four polystyrene microspheres.

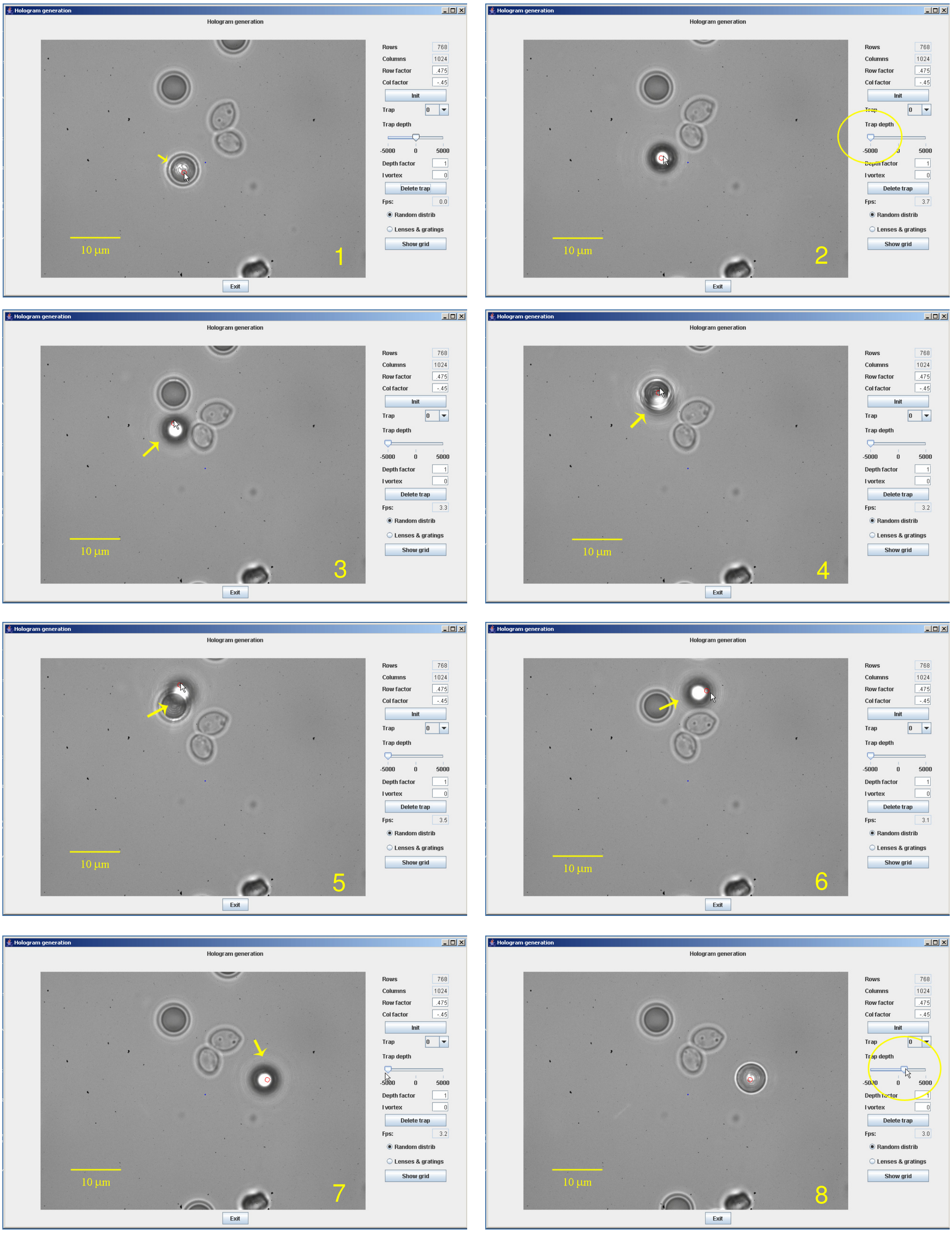

Fig. 9. Sequence of images showing trapping and manipulation in three dimensions.